OPEN AND CLOSED-LOOP EXPERIMENTS TO REATTACH A THICK TURBULENT BOUNDARY LAYER

T. Shaqarin[1], C. Braud[1,3], S. Coudert[1,3], M. Stanislas[1,2]

Univ Lille Nord de France[1] F-59000 Lille, EC Lille[2], CNRS[3],
Laboratoire de Mécanique de Lille (UMR 8107)
Boulevard Paul Langevin,
59655 Villeneuve d'Ascq Cédex,
France.
corresponding author: caroline.braud@univ-lille1.fr

ABSTRACT

Open and closed-loop control experiments were successfully performed to reattach a thick turbulent boundary layer, thanks to large scales of the facility (i.e. wind tunnel Carlier & Stanislas (2005)). This extends to large Reynolds numbers and large time scales the range of flow conditions for which open and closed-loop control configurations were investigated for turbulent flow separation configurations. Experiments were performed at three Reynolds numbers based on the momentum thickness of the turbulent boundary layer, varying from $Re_\theta \simeq 7500$ to 12600. First open-loop tests were conducted to identify the systems. They were found to behave like a first order linear one, with coefficients that need to be adapted depending on the Reynolds number. Then, simple controllers (Proportional-Integral and Linear Quadratic Regulator) were implemented in closed-loop configurations. They were able to significantly improve the reactivity of the system and consequently the cost of the control. A test of robustness was performed from variations of the free-stream velocity which highlights the need to improve it using more complex controllers.

1 Introduction

In the last decades many different flow control configurations (flat plates, ramps, bumps, ducts, airfoils, wind turbines ....etc) were investigated to delay or prevent turbulent boundary layer separations. Early studies using passive devices have demonstrated the influence of many geometrical parameters on the control efficiency (see e.g. Lin (2002)). Also, the flow in which the devices are embedded influences the dynamics of the produce vortices. Therefore, depending on the flow configuration, the optimal control parameters vary. To adapt the control to the flow situations passive devices were rapidly replaced by active devices. Many active device types were then developed for which, depending on the control source used, the control is of different nature (acoustic actuators, plasma actuators, fluidic actuators ...). When fluidic round jets are slanted relatively to the wall and to the main stream of the baseline flow, they are able to generate streamwise vortices, qualitatively similar than the so-called Vortex Generator (VG) actuators, which can entrain high-momentum fluid towards the wall, hence energizing the turbulent boundary layer, increasing quantities such as wall shear stress, turbulence intensities, momentum transfer, etc ... and delaying separation. The operating operators of the active devices (i.e. pulsating frequency, duty cycle, amplitude of the jet) were recently used in closed-loop configurations to demonstrates its ability to further decrease the cost of the control or/and to make it more robust (see e.g. Allan *et al.* (2000); Becker *et al.* (2007); Henning & King (2005); Benard *et al.* (2010)). Controllers using models which represents turbulent flow separations are generally of high dimension and need a high computational time which limits real time experimental implementations. Model-free approaches such as extremum seeking (Becker *et al.* (2007)), slope seeking (Benard *et al.* (2010)) or simple linear models limited to the tested configuration such as PID (Allan *et al.* (2000)) were thus generally preferred. However, they are limited to the tested configurations (airfoils Benard *et al.* (2010), backward facing-step Henning & King (2005) ...). To improve the fundamental understanding of the separation mechanisms, some studies have extracted the transient time when going from the two states of the flow (i.e. separated/attached) (Amitay & Glezer (2002); Darabi & Wygnanski (2004); Mathis & Bonnet (2009); Siauw *et al.* (2010)). The understanding of such mechanisms will enable to improve significantly the control robustness. Unfortunately, this time scale is not systematically reported by closed-loop studies and more experiments are needed over a larger spectrum of separated configurations.

In the present work, a thick turbulent boundary layer is generated on an inclined ramp, which produce a slight adverse pressure gradient coefficient dC_p/ds =0.06 before a separation. Thanks to the large scales of the facility (i.e. wind tunnel Carlier & Stanislas (2005)), this extends to large Reynolds numbers and large time scales the range of flow conditions for

which open and closed-loop control configurations are investigated. In a previous set of experiments (Cuvier *et al.* (July 2011)), a parametric study was conducted to choose the optimal actuator arrangements (exit hole geometry, spacing between jets, orientations ...) at the highest Reynolds number $Re_\theta = 12600$. In the present study, open loops experiments were first performed to extract the dynamic of the systems for three Reynolds numbers based on the momentum thickness of the turbulent boundary layer, varying from $Re_\theta \simeq 7500$ to 12600, and their associated time scales. Then, simple controllers (Proportional-Integral and Linear Quadratic Regulator) were implemented in closed-loop configurations to get a better reactivity of the system and to improve the robustness under variations of the free-stream velocity.

2 LML Wind tunnel facility and the model

The experiments were conducted in the boundary layer Wind Tunnel of "Laboratoire de Mécanique de Lille" (LML). The LML wind tunnel is extensively described and characterized in Carlier & Stanislas (2005). The working section is 1 m high, 2m wide and 21.6 m long. The flow is produced by a fan and a motor that allow the variation of the free-stream velocity U_∞ from 3 m/s to 10 m/s with a stability better than 0.5%. The turbulence level in the free stream is about 0.3% of U_∞, and the temperature is kept within $\pm 0.2C^\circ$ by use of an air-water heat exchanger in the plenum chamber. The turbulent boundary layer under study develops on the lower wall of the working section after being tripped at the entrance by a grid fixed on the floor. The long length of the working section ($21.6\,m$ at most) induces a thick turbulent boundary layer: around $0.3\,m$ at the entrance of the test section. A ramp model was added in the test section. It is composed of four parts (figure 1). First, a smooth converging part with a contraction ratio of 0.75 is needed to generate an adverse pressure gradient in the following part. The second part is an articulated flat plate that can rotate from $\alpha = 2^\circ$ to $\alpha = -4^\circ$ around its leading edge. For $\alpha = 0^\circ$ the flat plate is parallel to the streamwise direction. The third part is also an articulated flat plate and will be called later flap. It can rotate from $\beta = -5^\circ$ to $\beta = -40^\circ$ around its leading edge. Finally, the fourth part of the model consists of a flexible sheet of PVC that is shaped to obtain a smooth transition with the wind tunnel floor.

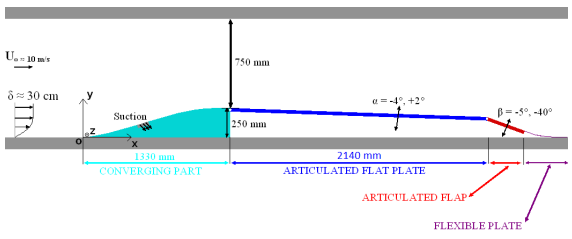

Figure 1. Schematic view of the model.

As shown in previous results (Cuvier *et al.* (July 2011)), by adjusting α, a favorable, adverse or zero pressure gradients can be obtained on the flat plate. Also, for $\beta = -19$, a separation occurs on the flap which is 2D over 70% of its span. In the present study the flat plate is set to $\alpha = -2$, generating an adverse pressure gradient and the flap is adjusted to $\beta = -22^\circ$. The origin of the coordinate system is located on the lower wall, at the mid-span, at the beginning of the converging part, corresponding to a distance of 14.4m from the tripping device. The separation line is at $s = 3500$ mm at the intersection between the flat plate and the flap. The separation length, was roughly estimated from wool tufts visualisation to $L_{sep} \approx 0.8$m. For this configuration the boundary layer thickness is approximatly 20 cm before separation and the pressure gradient is dC_p/ds=0.06. Experiments were conducted at three Reynolds numbers (from $Re_\theta \simeq 7500$ to $\simeq 12600$ or for three free-stream velocities $U_\infty = 5$, 8 and 10m/s).

3 Actuators

3.1 Geometrical arrangement

To generate streamwise vortices similar to the ones obtained from passive devices (Godard & Stanislas (2006)), round jet orifices were inclined relatively to the wall and to the flow. In the present study, only tunable parameters that can be used in closed-loop implementations are varying and the others are fixed from previous optimizations of Cuvier *et al.* (July 2011) of the same configuration. A spanwise line of 22 co-rotating jets of diameter Φ =6mm was placed on the flat plate upstream of the separation at $s = 3219$ mm. They were inclined by 135° relatively to the free-stream velocity (i.e. blowing upstream) and by 45° from the wall. Jets were located 47Φ upstream of the separation line and their axis were spaced by 13.6Φ from each others.

3.2 Apparatus to pulse the jets

Contrary to passive devices, the control depends strongly on the perturbations delivered by the actuator which is a result of the flow produced inside the device and, in most of experimental investigations, the actuator validity and limitations are not properly known (Cattafesta & Sheplar (2011)). In the present work, a specific apparatus was used to pulse the jets. It is composed of a reservoir, a solenoid valve, a throat which creates a sonic orifice and a tube. The air is supplied in a reservoir at pressure p_r and flows through the valve, the throat and then along a tube of diameter Φ. It is discharged into the atmosphere at constant pressure p_o. The throat section S_c, is small with respect to the tube section $S = \pi\Phi^2/4$. These actuators can be operated continuously with the valves open or can be pulsed by switching the valves ON and OFF alternatively. The velocity at the exit of the tube for these two operating modes was modeled by Braud & Dyment (2011). This offers the ability to fix and optimize the working conditions of the actuator, according to criteria defined in advance. In the continuous mode, the exit velocity is characterized by the small dimensionless parameter $S_c p_r/(Sp_o)$. In the pulsed mode, characterized by the time scale L/c_o, the exit velocity is driven by two dimensionless parameters, the same as in the steady state $S_c p_r/(Sp_o)$ and by L/D. Hence, the working conditions can be set by adjusting the parameters $S_c p_r/Sp_o$ and L/D. In the present work two nozzles were designed with two different throat diameters 0.8mm and 1.3mm which per-

mits to stay within the assumptions of the model and thus to have a perfect knowledge of the transfer function of the actuators. A fixed delay of 1ms exists at the opening of the valve, it adds to a delay which depends on the tube length equal to $L/c_o = 0.6$ ms for the present experiments using a length of $L = 20$cm.

3.3 Air circuit

The air circuit which was used to provide compressed air to the actuators is composed of a compressor, a filtration system, a proportional valve, two volumetric flow meters (Q_v), a manometer (p_r), a thermometer (T_r) and a large reservoir of 90 liter. The main purpose of this circuit is to adjust and measure the velocity at the exit of the actuators. The proportional valve adjust the exit velocity, while its mean value is obtain through the measurement of the mass flow rate ($Q_m = Q_v * p_r/RT_r$ with $R = 287$J/(Kg.K)) using the mass conservation, $Q_m = \rho_j S_j U_j N_j$, with ρ_j the density of air at the exit of the actuator, S_j the cross section of the jet, U_j the mean velocity at the exit of the jet and $N_j = 22$ the number of jets. For incompressible jets, the temperature and pressure at the exit of the jet are equal respectively to the ambient temperature T_a and pressure P_a. Hence, the mean exit velocity of the actuator is given by $U_j = \frac{Q_v p_r}{S_j N_j P_a}$.

4 Sensors

Detecting the separation of a turbulent flow is always a difficult task as the separation is unsteady. Moreover, in the present facility, it occurs over a large domain that cannot be simply covered using classical techniques (PIV, hot-wire, LDV, hot-films ...). In the present study, it was decided to have both a global overview of the flow separation using wool tufts and a local measure using hot-films on the flap. This combination provides a quick assessment of the control efficiency. The hot-film probe is sensitive to the absolute value of the skin friction $|\tau|$. Under control action, the skin friction gain increases, i.e. $|\tau|-|\tau_0| > 0$ with $|\tau_0|$ the skin friction in the non-actuated case (Godard & Stanislas (2006); Cuvier *et al.* (July 2011)). Above a certain level of the gain in skin friction, estimated from the wool tufts visualizations, the flow is attached. In the following, the gain in voltage $E - E_o$ will be used instead, since non-linearities introduced by the calibration make the control implementation more complex without reasons. At $U_\infty = 5$m/s the flow is attached for $E - E_0 = 0.035$V and this value increases when the free-stream velocity increases. One hot film probe (Senflex SF9902) was placed on the flap close to the separation line at $s = 3555$ mm, in the wake of a produced streamwise vortex at $z = 164$ mm. The probes were connected to a constant temperature anemometer AN 1003 manufactured by AAlabSystems.

5 Control set-up

Two measurement chains were set-up. One for open-loop experiments which separates the management of signals from the actuators and sensors. And one closed-loop which is using the hot-film signal, $E - E_0$, to drive the valves. In both configurations, the signal from the hot-film probe was digitized at a sampling frequency f_{aq} using a PCI-DA56036 acquisition board and an anti-aliasing filter with a cutting frequency f_c ($f_{aq} = 20$khz and $f_c = 5$khz in open-loops; $f_{aq} = 200$Hz and $f_c = 50$Hz in closed-loops). Valves are closed or open using a signal of respectively 0 and 24 Volts. Therefore, they can be pulsed using a square wave signal from 0 to 24 volts, allowing to define the Duty Cycle $DC = t_h f$ with t_h the opening time and f the pulsating frequency. This signal is provided independently using a ATmega1280 micro-controller to avoid any time delay and is recorded with the above data acquisition system for synchronization purposes. In open-loop tests, the desired Duty Cycle is set through the micro-controller before the acquisition is performed. In closed-loop configurations, the micro-controller is set so that it send a square wave signal with a Duty Cycle proportional to a continuous signal provided by the output of the acquisition board. It was checked that a control order can be sent every 10ms without any jitters from the management of the operating system. This control speed was found fast enough compared to the time scales of the separation/reattachment mechanisms of the present configuration (see section 6.1.2). The square wave signal is then distributed towards the 22 solenoid valves using electronic rapid commutation components. The control laws that provides the continuous signals to the micro-controller are implemented in C++ home made programs. When using the DC as an input variable, an additional digital low pass filter is needed to remove oscillations due to the actuation frequency in the input variable. Therefore, the minimum duration between two control actions was limited by the value of the pulsating frequency f.

6 Results

Open-loop tests were performed to define the best input/output variables, to extract time scales of the system and to identify it. Based on these results closed-loop experiments were performed with different objectives. The first one is to reattach the flow with the best reactivity and the minimum control expense. The second one is to keep the flow attached while the system is perturbed with variations of the free-stream velocities.

6.1 Open-loop

The system to control is composed of the actuators, the flow over the ramp and the sensors. Open loop tests performed in the present work are described as follows: departing from the separated baseline configuration, the valves are suddenly opened at a given value of the input variable, u, during 5 seconds, then they are suddenly closed. When using the DC as an input variable, measurements are repeated 100 times and are phase-averaged. The response of the system to this step function was observed through the chosen output variable, y. The opening time is chosen long enough to stabilize the dynamic response of the system in its steady state, y_{ss}. When the chosen input variable is $VR = U_j/U_e$ with U_e the local free-stream velocity, the steady state corresponds to continuous mode of the actuator. This procedure enables to extract the transfer function of the separation/reattachment dynamic process.

6.1.1 Input/output variables

The state of the flow is given through the signal $y(t) = E(t) - E_0$ from the hot-

film probe located smartly on the flap (see section 4) using previous results of Cuvier *et al.* (July 2011). By manipulating VR, it is possible to act on the output variable. Moreover, the steady state value of the hot-film signal was found linearly proportional to VR. Thus, as a first approach, VR could be considered as an appropriate input variable for closed-loop implementations. However, varying dynamically VR limits the time between two control actions due to the inertia of the compressed air circuit. Therefore, the DC candidate was explored instead, as suggested by Kostas *et al.* (2009). Indeed, the strength of the streamwise vortices and thus the ability to reattach the flow being proportional to the mass flow rate, a similar result should be obtained by varying either VR in the continuous mode, or DC in the pulsed mode. Moreover, when using the DC as an input variable, the minimum duration between two control actions, given by $1/f$, can be reduced to around 3ms when using the present valves. The ability of this variable to be used as an input variable for closed-loop implementations was checked for all the Reynolds numbers investigated. For that purpose, different values of DC were set using a fixed value of $VR = 3.6$ and a time step of the control action around 0.1s (i.e $f = 15$Hz). Under these conditions, the flow attached for $DC > 50\%$. A step function was then sent to the system by a sudden opening at a given DC during 5 seconds and then the valves are suddenly closed. Results show that DC is able to control the output variable $E - E_0$ and thus the state of the flow, with an affine relationship between them (see e.g. figure 2 for $Re_\theta = 7500$ using $U_\infty = 5$m/s). This will be the input variable used for all the following control experiments.

6.1.2 System identification and time scales The response of the system to a step function was observed for three free-stream velocities (5, 8 and 10 m/s). The pure delay t_{Delay} observed at the beginning of the step responses has two origins: the first one is the delay of the actuators which is of the order of 1.6 ms (section 3.2), the second one is the time necessary for the input signal to be convected towards the output signal through the system t_{conv}. From the measurement of t_{conv} a convective velocity U_{conv} can be estimated using the Taylor hypothesis $t_{conv} = L_{conv}/U_{conv}$ with $L_{conv} = 0.44$m the distance between the actuator and the hot-film probe. Structures produced from jets which are blowing upstream, traveled first in the turbulent boundary layer with a slight adverse pressure gradient and then in the separated area where complex mechanisms occurs. For $U_\infty = 5$,8 and 10 m/s the ratio U_{conv}/U_∞ is respectively 0.6, 0.4, 0.4. Hence they are convected at around half the free stream velocity while, assuming the flow is reattached by the actuator, the mass conservation in the diverging part of the bump leads to a reduction of around 2% of the free stream velocity.

After this pure delay, all systems are observed to behave like a first order linear system for both the attachment and separation process (see for instance figure 3). Therefore they will be modeled in the state space representation as follows:

$$\frac{dx(t)}{dt} = ax(t) + bu(t) \quad (1)$$

$$y(t) = cx(t) \quad (2)$$

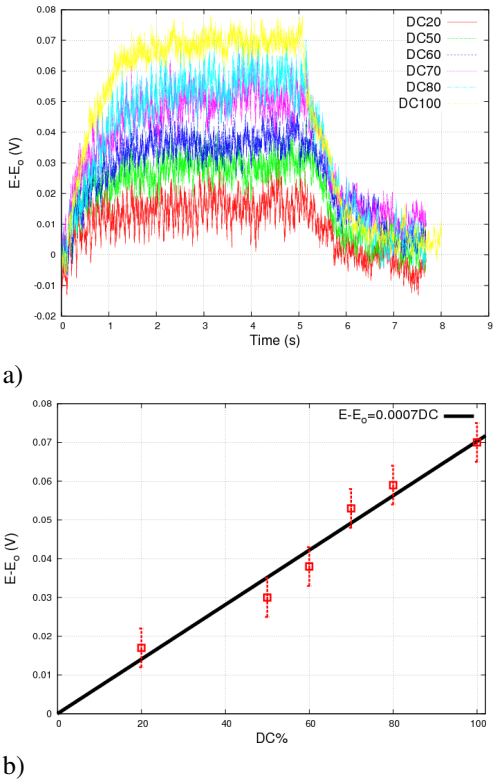

Figure 2. Open-loop response of the system using DC as an input variable and the hot-film probe number 1 as an output variable: a) to a step function and b) input/output relationship in the steady state.

with $x(t)$ the state of the flow, $u(t)$ the input variable (i.e. $DC(t)$), $y(t)$ the output variable (i.e. $E(t) - E_o$) and a, b constants obtained from a least square approximation between the open-loop response and the solution of the previous system while is set to $c = 1$. In the steady state (i.e. when $e^{At} \to 0$) the output variable is given by $y_{ss} = \frac{-u_i cb}{a}$. The relation between the steady state value of the output variable y_{ss} and the input variable u is linear as observed experimentally (figure 2b) and the slope, also called the steady state gain H, is given by $H = \frac{-cb}{a}$. The settling time $t_{set} = t_{99\%} + t_{Delay}$ is the time needed to reach 99% of y_{ss} with $t_{99\%}$ the time scale of the system without pure delay (figure 3). $t_{99\%}$ can be directly obtained from the knowledge of the coefficient a, $t_{99\%} = \frac{1}{a} ln(0.01)$.

The different systems corresponding to the attachment and separation process for the three Reynolds numbers were identified using the previous procedure. The obtained coefficients a,b and c are given in table 1 together with the time scale t_{set} and the steady state gain H for the same input variable $u_i = DC = 100\%$. Note that the time scale associated to both the separation/reattachment process are similar.

Thanks to large scales of the facility, the time scale t_{set} is much larger than the convective time t_{conv} and the time scale of the actuators, which will be both neglected in the following. In other words, the measured time scales t_{set} of the system through the open-loop tests will be assimilated to time scales of the separation/reattachment process. A dimensionless rep-

U_∞ [m/s]	a	b	Q_m [10^{-7} Kg/s]	t_{set} [s]	H	$t_{att}^+ = t_{sep}^+$
5	-1.74	0.001	1.64	2.65	0.00057	16.6
8	-2.46	0.0025	2.64	1.87	0.00101	18.7
10	-4.85	0.005	3.2	0.95	0.00103	11.9

Table 1. Summary of the time scales and steady state gains of the system for $VR \simeq 3.6$.

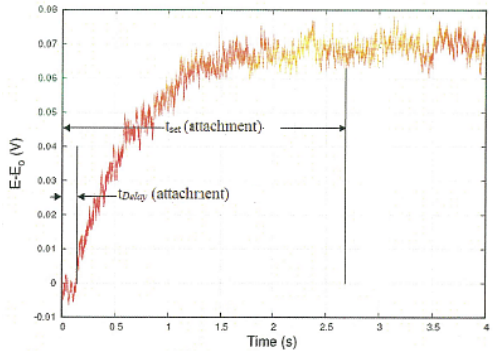

a)

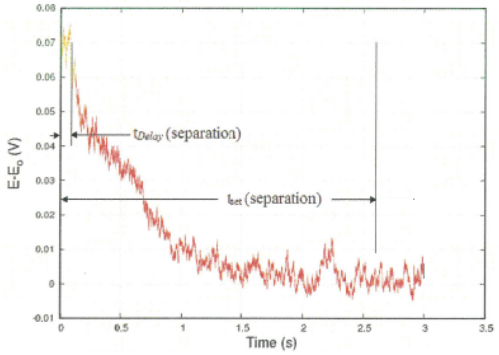

b)

Figure 3. Definition of the involved time scales from the open-loop response to a step function. t_{Delay} is a pure delay at the opening of the actuators and $t_{set} = t_{Delay} + t_{99\%}$ is the settling time with $t_{99\%}$ the time scale of the: (a) attachement process and (b) separation process (the origin is the closure of the valve).

resentation of the time scales t_{set} similar to the one used in other studies Amitay & Glezer (2002); Darabi & Wygnanski (2004); Mathis & Bonnet (2009); Siauw *et al.* (2010) can be expressed for sake of comparison, i.e. $t_{att}^+ = t_{sep}^+ = t_{set} U_\infty / L_{sep}$ with $L_{sep} = 0.8$m the estimated length of separation (see table 1). The attachment time is found larger in the present study while the separation time is of the same order of magnitude. This indicates that the mechanisms associated to reattachment of the flow are different while the separation mechanisms seems to be similar. Actuators are supposed to be at the origin of the differences as, for this last mechanism, they are turned off. In particular, the orientation of the present actuators, which are blowing upstream, leads naturally to a smaller reactivity of the system as the relative velocity is lower. However, more investigations are needed to conclude on this subject as several other factors may be involved such as the initial state of the flow (i.e. attached or separated), the actuator type and the flow configuration ...

6.2 Closed-loop

Using the same input/output variables as in open-loop systems, simple linear controllers were implemented to improve the control reactivity and to test the robustness of the control under variations of the free stream velocity.

6.3 Controllers

First a Proportional Integral (PI) controller was implemented using the following differential form $\frac{du}{dt} = k_i e + k_p \frac{de}{dt}$, discretized using backward finite differences. Then, a Linear Quadratic Regulator (LQR) controller was implemented (Van.De.Vegte (1994)). The objective of this controller is to give the best trade-off between performance and cost of control. It is formulated to minimize J given by $J = \int_0^\infty (x^T Q x + u^T R u)$, with $x^T Q x$ and $u^T R u$ representing respectively a measure of the control efficiency and the control cost. The choice of the coefficients Q and R allows the relative weighting of state variables and control inputs. Increasing Q relatively to R improves the control efficiency while the cost of the control is increased. The Choice of Q and R requires considerable trial and error until the transient response is satisfactory. The optimal control is then implemented using a constant-gain state feedback as follows $u = -Kx$ with $K = R^{-1} B^T P$, where P is a symmetric and positive definite matrix obtained from the solution of the algebraic matrix Riccati equation $PA + A^T P + Q - PBR^{-1} B^T P = 0$.

6.3.1 Reactivity

Starting from the separated flow on the flap, the objective of the control was to reattach the flow at a minimum cost with the fastest reactivity. The flow is observed to be attached for $DC > 50\%$. The objective of the control is to target $DC = 50\%$ so that the flow is just attached (i.e. optimal in term of the control cost). Therefore, the reference value is fixed and is given by $r = DC = 50\%$. Figure 4 gives respectively the output variable and the output of the controller (i.e. input variable) using P, I, and LQR controllers for one Reynolds number $Re_\theta = 7500$ (i.e. $U_\infty = 5$m/s) and a fixed value of $VR = 3.6$ and of the pulsating frequency $f = 15$Hz.

Compared to open-loop results, P and LQR controllers were equally able to improve the reactivity of the system by more than three times. Indeed, as shown for one Reynolds

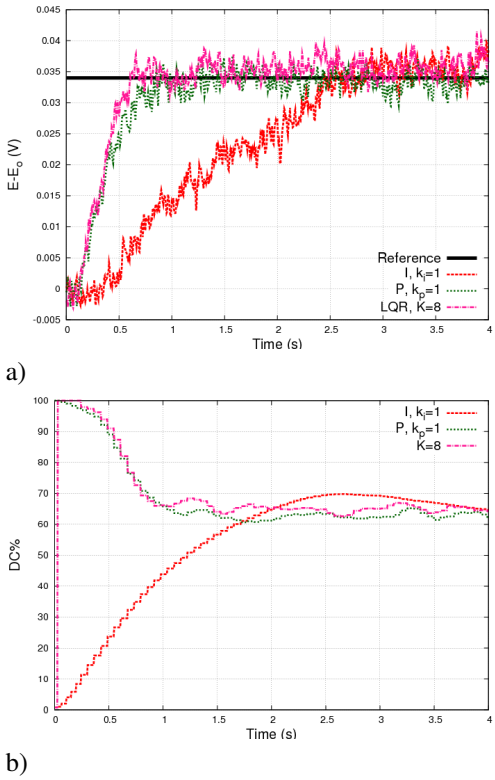

Figure 4. Response of the closed-loop system using different type of controllers (P,I, PI and LQR) for $U_\infty = 5$m/s, a fixed value of $VR = 3.6$ and of the pulsating frequency $f = 15$Hz: a) Output variable and b) Input variable.

number $Re_\theta = 7500$ in figure 4a, $t_{set} = 0.8$s while in the open-loop configuration $t_{set} = 2.65$s. For the I controller no improvement of the reactivity could be found. For the two successful controllers, the maximum value of the input variable or control output is reached, i.e. $u = 100\%$, during the first instant (figure 4b) with the same cost of the control (i.e. integral of the DC value over time). The maximum control effort occurs during about 0.8s which corresponds to 30% of the time scale of the open-loop system $t_{set} = 2.65$s. In the closed-loop, the steady state value is reached at arround $t_{set} = 0.8$s with the maximum of the input variable $DC = 100\%$ while, in the open-loop, the same steady state is obtained at $t_{set} = 2.65$s with $DC = 50\%$. Due to the short time action of the closed-loop configuration, this represents a gain in term of cost of the control. It can be quantified using the duty cycle times the settling time, $DC * t_{set}$, which is almost twice smaller in the closed loop configuration.

These results show that the closed-loop configuration improves both the control reactivity and the cost of the control by the introduction of more mass flow at the first instant of the control action. In the present experiments the maximum control output was reached during these first instant using valves in the continuous mode $u = DC = 100\%$ and $VR = 3.6$. A higher mass flow can be obtain by increasing VR. Therefore, to improve the reactivity and the cost of the control of the system, the simplest way would be to have an initial value of VR higher than $VR = 3.6$. VR being related by a linear law to the inlet pressure in the reservoir of the valve p_r, this is equivalent to increase this pressure. However, over a certain threshold of VR, the jets may be produced outside the boundary layer thickness which would induce both additional drag penalty and a reduction of the control efficiency. This threshold was not reached in the present experiments due to limitation of the valves.

6.3.2 Robustness

Departing from the flow separated on the flap at $U_\infty = 5m/s$ and the best previous controller, i.e. P controller with $k_p = 1$, perturbations were introduced throught variations of the free-stream velocity in the following range U_∞, $4.2m/s < U_\infty < 5.8m/s$ (figure 5a). An ideal controller would keep the output variable at the desired state, $E - E0 \simeq 0.035$, during the perturbation of the system. As can be shown in the response of the output variable, the P controller fails for this task during the perturbations (figure 5b). However, once the perturbation is gone, the control goes back to the reference value. Hence, the P controller perfomances are half sucessfull.

It can be noticed that the input variable starts to go back to the reference value at $t = 7$s and $t = 15$s, before the perturbation changes its evolution at respectively $t = 10$s and $t = 17$s. Indeed, from the observation of the control output (figure 5c), its action progressively increases until a certain threshold at $t = 7$s or $t = 15$s, which is found enough to have a reaction of the system. It is therefore sought that, as soon as small perturbations of the free stream velocity are detected, a strong level of control output during a short period of time would be more appropriated to maintain the output variable at the desired reference value. Of course a compromise has to be found to avoid the instability of the controlled system. This could be reached by using some modifications of the P controller or by using a more appropriate one.

7 Conclusion

Flow separation control experiments were performed on a ramp with a particularly thick turbulent boundary layer before separation, $\delta \simeq$ 20 cm, which induces high Reynolds numbers and large time scales. Thanks to the specific characterics of the present facility, the input variable (i.e. Duty Cycle), was able to sent a control action at least 10 times faster than the time scales of the separation/reattachement process. The chosen output variable was the voltage signal from a hot-film probe placed smartly on the flap to represent the two states of the flow (i.e. attached/separated). The control objective was to reattach the flow in the separated region with the minimum of mass flow rate. Open-loop tests were performed to identify the dynamic of the system and their time scales for three Reynolds numbers based on the momentum thickness of the turbulent boundary layer, varying from $Re_\theta \simeq 7500$ to 12600. They were found to behave like a first order linear one, with coefficients that need to be adapted depending on the Reynolds numbers. Time scales were found to decrease linearly when the Reynolds is increasing from $t_{set} = 2.65$s to 0.98s (dimensionless time scale from $t^+ \simeq 11.9$ to 16.6).

Based on this analysis, different closed-loop controllers were implemented (Proportional, Proportional and Integral, and Linear Quadratic Regulator). Two objectives were tar-

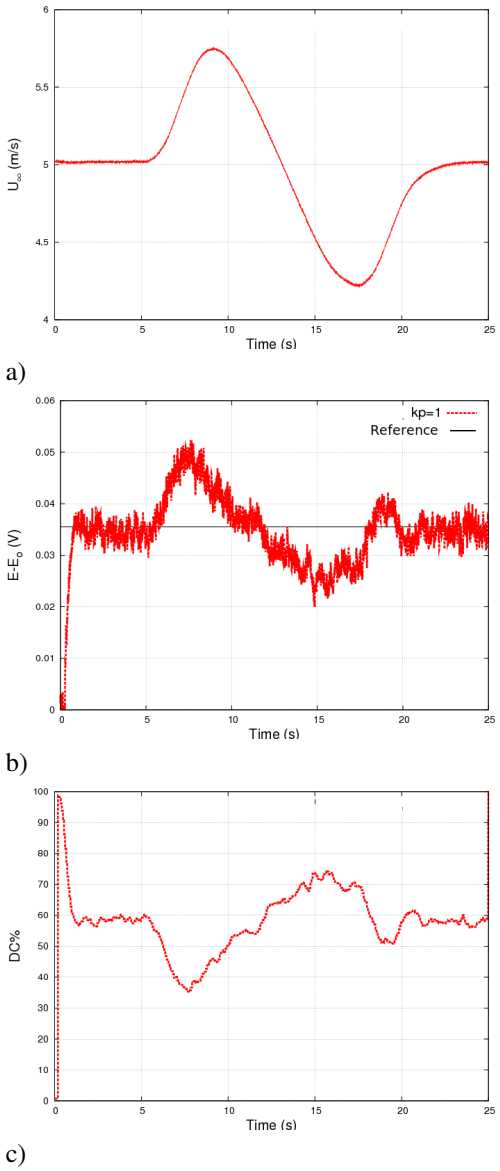

Figure 5. Response of the closed-loop system when perturbed by variations of the free-stream velocity: a) Perturbations, b) Output variable and c) Input variable.

geted: the first one was to reattach the flow with the minimum of mass flow rate and the maximum of reactivity, the second was to test the robustness of the control under variations of the free-stream velocities. Closed-loop configurations were able to increase the reactivity by more than 3 times than open-loop tests with an additional gain in term of mass flow rate. The controller was found robust to maintain the desired state of the flow under variations of the free-stream velocity with, however, a larger delay in the time reactivity that needs to be improved. Future work will aim at improving the robustness of the closed-loop system for separated flows.

REFERENCES

Allan, B. G., Juang, J., Raney, D. L., Seifert, A., Pack, L. G. & Brown, D. E. 2000 Closed-loop separation control using oscillatory flow excitation. *Tech. Rep.*. NASA/CR-2000-210324, ICASE Report 2000-32.

Amitay, M. & Glezer, A. 2002 Controlled transient of flow reattachment over stalled airfoils. *Int. J. Heat Fluid Flow* **23**, 690–699.

Becker, R., King, R., Petz, R. & Nitsche, W. 2007 Adative closed-loop separation control on a high-lift configuration using extremum seeking. *AIAA* **45**, 1382–1392.

Benard, N., Moreau, E., Griffin, J. & Cattafesta, L. 2010 Slope seeking for autonomous lift improvement by plasma surface discharge. *Experiment in Fluids* **48**, 791–808.

Braud, C. & Dyment, A. 2011 Model of an impulsive actuator for flow control applications. *submitted* .

Carlier, J. & Stanislas, M. 2005 Experimental study of eddy structures in a turbulent boundary layer using particule image velocimetry. *Journal of Fluid Mechanics* **535** (36), 143–188.

Cattafesta, L. & Sheplar, M. 2011 Actuators for active flow control. *Annual Review of Fluid Mechanics* **43**, 24772.

Cuvier, C., Braud, C., Foucaut, J.M. & Stanislas, M. July 2011 Flow control over a ramp using active vortex generators. In *Proceedings of the Seventh Internationnal Symponium on Turbulence and Shear Flow Phenomena*.

Darabi, A. & Wygnanski, I. 2004 Active management of naturally separated flow over a solid surface. part 1. the forced reattachment process. *J. Fluid Mech* **510**, 105–129.

Godard, G. & Stanislas, M. 2006 Control of a decelerating boundary layer. part 3: Optimization of round jets vortex generators. *Aerospace Science and Technology* **10** (6), 455–464.

Henning, L. & King, R. 2005 Multivariable closed-loop control of the reattachment length downstream of a backward-facing step. In *16th IFAC World Congress*. Praha, Czech Rep.

Kostas, J., Foucaut, J.M. & Stanislas, M. 2009 The effects of pulse frequency and duty cycle on the skin friction downstream of pulsed jet vortex generators in an adverse pressure gradient turbulent boundary layer. *Aerospace Science and Technology* **13**, 3648.

Lin, J.C. 2002 Review of research on low-profil vortex generators to control boundary layer separation. *Progress in Aerospace Sciences* **38**, 389–420.

Mathis, R. & Bonnet, J.P. 2009 Experimental study of transient forced turbulent separation and reattachement on a bevelled trailing edge. *Experiments in Fluids* **46**, 131–146.

Siauw, W.L., Bonnet, J.-P., Tensi, J., Cordier, L., Noack, B.R. & c, L. Cattafesta 2010 Transient dynamics of the flow around a naca 0015 airfoil using fluidic vortex generators. *Journal of Turbulence* **31**, 45–459.

Van.De.Vegte, J. 1994 *Feedback Control Systems*. New Jersey, Prentice-Hal.